Janiszewski, Mateusz; Shen, Baotang; Rinne, Mikael

Simulation of the interactions between hydraulic and natural fractures using a fracture mechanics approach

Published in:
Journal of Rock Mechanics and Geotechnical Engineering

DOI:
10.1016/j.jrmge.2019.07.004

Published: 03/12/2019

Document Version
Publisher's PDF, also known as Version of record

Journal of Rock Mechanics and Geotechnical Engineering 11 (2019) 1138–1150

Contents lists available at ScienceDirect

Journal of Rock Mechanics and Geotechnical Engineering

journal homepage: www.rockgeotech.org

Full Length Article

Simulation of the interactions between hydraulic and natural fractures using a fracture mechanics approach

Mateusz Janiszewski[a,*], Baotang Shen[b], Mikael Rinne[a]

[a] Department of Civil Engineering, School of Engineering, Aalto University, PO Box 12100, FI-00076 AALTO, Espoo, Finland
[b] CSIRO Energy QCAT, 1 Technology Court, Pullenvale, Australia

A R T I C L E I N F O

Article history:
Received 16 October 2018
Received in revised form
4 February 2019
Accepted 25 April 2019
Available online 1 August 2019

Keywords:
Hydraulic fracturing
Fractured rock
FRACOD model
Underground thermal energy storage
HYDROCK
Artificially fractured hard rock aquifer
Granite

A B S T R A C T

HYDROCK method aims to store thermal energy in the rock mass using hydraulically propagated fracture planes. The hydraulic fractures can interact with the pre-existing natural fractures resulting in a complex fracture network, which can influence the storage performance. This study investigates the interactions between hydraulic and natural fractures using a fracture mechanics approach. The new functionality of the fracture mechanics modelling code FRACOD that enables crossing of hydraulically driven fracture by a pre-existing fracture is presented. A series of two-dimensional numerical models is prepared to simulate the interaction at different approach angles in granitic rock of low permeability. It is demonstrated that multiple interaction mechanisms can be simulated using the fracture mechanics approach. The numerical results are in agreement with the modified Renshaw and Pollard analytical criterion for fracture crossing. The results show that for large approach angles, the hydraulic fracture crosses the natural fracture, whereas for small approach angles, the hydraulic fracture activates the natural fracture and the wing-shaped tensile fractures are propagated from its tips. Thus, the presence of fractures with low dip angles can lead to the growth of more complex fracture network that could impair the thermal performance of the HYDROCK method.

1. Introduction

The intermittent nature of some renewable energy sources derives from their over-supply during the low season and under-supply during the peak season. The solution is to accumulate and store the surplus energy seasonally and use it in times of high demand and low supply. HYDROCK is a method for storage and extraction of thermal energy in an artificially fractured hard rock aquifer developed in Sweden (Eriksson et al., 1983; Larson et al., 1983; Larson, 1984; Sundquist and Wallroth, 1990; Hellström and Larson, 2001). The HYDROCK method requires multiple parallel horizontal fracture planes to be constructed in the rock mass using the hydraulic fracturing technique. The method is feasible in areas characterised by reverse faulting stress regime, where hydraulic fracturing in vertical boreholes will produce sub-horizontal fracture planes (Hellström and Larson, 2001). Thermal energy is then charged into the rock mass by pumping hot fluid through artificially fractured aquifer, as shown in Fig. 1. Recent experiments have shown that a reduction of 50% in the construction cost could be achieved by using hydraulically fractured aquifer compared to conventional methods that use borehole heat exchangers (Ramstad, 2004; Ramstad et al., 2007; Liebel et al., 2012).

Hellström and Larson (2001) suggested that for an ideal HYDROCK system to provide 2 GW h of energy per season, 25 parallel fracture planes of 25 m radius at 2 m spacing are required. In addition, a sufficient hydraulic conductivity of the induced fractures is required to facilitate the hydraulic connection between the injection and extraction wells. Thus, the overall success of HYDROCK is reflected by the ability to construct a system with a sufficient number of parallel, induced fracture planes of a sufficient radial extent and hydraulic conductivity.

Hydraulic fracturing was first introduced for stimulation of wells in oil reservoirs (Clark, 1949). Since then, it has been used extensively for the extraction of shale gas (Wang et al., 2014), extraction of water from hard crystalline rocks (Less and Andersen, 1994; Joshi, 1996; Cobbing and Dochartaigh, 2007; dos Santos et al., 2011; Hart, 2016), and reservoir stimulation of enhanced

* Corresponding author.
E-mail address: mateusz.janiszewski@aalto.fi (M. Janiszewski).

Peer review under responsibility of Institute of Rock and Soil Mechanics, Chinese Academy of Sciences.

https://doi.org/10.1016/j.jrmge.2019.07.004

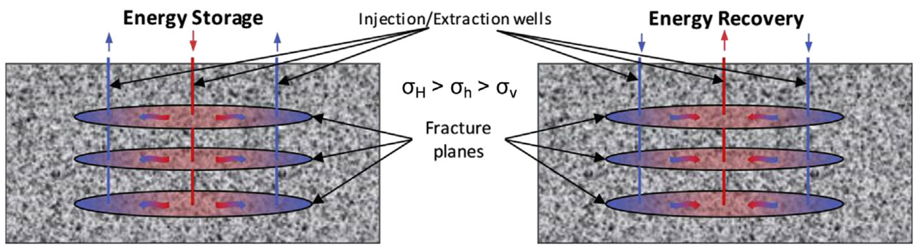

Fig. 1. Schematic diagram of the HYDROCK thermal energy storage method. The method is feasible in reverse faulting stress regime, where hydraulic fracturing in vertical boreholes will produce sub-horizontal fracture planes. During the heat storage phase, the heat carrier liquid is pumped into the central hole, flows through sub-horizontal fracture planes towards the peripheral holes and heats up the surrounding rock. During the extraction phase, the cycle is reversed.

geothermal systems (Pine and Batchelor, 1984; McClure and Horne, 2014; Olasolo et al., 2016). Other applications include in situ rock stress measurements (Amadei and Stephansson, 1997) and pre-conditioning of rock in block cave mining (He et al., 2016). Hubbert and Willis (1957) first postulated that the orientation of an induced hydraulic fracture follows the path of least resistance. Thus, it initiates in the plane perpendicular to the axis of the minimum principal in situ rock stress. However, away from the drill hole, a fracture driven by fluid flow is influenced by the local geology and the hydraulic fracture may alter its orientation if discontinuities or flaws disturb the local stress orientation. Fracture branching, offset crossing and non-planar fracture growth were frequently observed in laboratory and field experiments on hydraulic fracturing in rocks with pre-existing discontinuities (Lamont and Jensen, 1963; Blanton, 1982, 1986; Warpinski and Teufel, 1987; Jeffrey, 1996; Cheng et al., 2014; Dehghan et al., 2015).

In view of that, the presence of the pre-existing fractures in the rock mass may arrest or divert the induced hydraulic fracture leading to a more complex fracture network in comparison with the ideal, sub-horizontal fracture planes as assumed in the HYDROCK concept presented by Hellström and Larson (2001). Therefore, understanding of the complex interaction mechanisms between hydraulic and natural fractures is necessary for a successful implementation of the HYDROCK method.

Many authors provide analytical models capable of predicting whether the crossing of a natural fracture by an induced fracture will occur based on laboratory observations (Blanton, 1982, 1986; Warpinski and Teufel, 1987; Renshaw and Pollard, 1995; Gu and Weng, 2010; Cheng et al., 2014; Liu et al., 2014; Sarmadivaleh and Rasouli, 2014). The criteria are based on several factors, such as the differential stress, the approach angle between the hydraulic and natural fractures, and the properties of the pre-existing fracture. Sarmadivaleh and Rasouli (2014) provided a comprehensive summary of the available analytical criteria for fracture crossing.

However, due to the inherent complexity of the hydraulic fracturing process and the interactions between induced and pre-existing fractures, laboratory investigations and analytical criteria have limited applicability attributable to their inherent assumptions and simplifications. Therefore, numerical methods that enable hydro-mechanical (HM) coupling of the fluid flow and the mechanical response of the rock mass are used extensively to simulate the hydraulic fracturing process in the presence of pre-existing discontinuities. The commonly used numerical methods for simulation of hydraulic fracturing in fractured rock masses include the finite element method (FEM) (e.g. Xu et al., 2015), the extended finite element method (XFEM) (e.g. Dahi-Taleghani, 2009; Shi et al., 2017), and the boundary element method (BEM) including the displacement discontinuity method (DDM) (e.g. Zhang and Jeffrey, 2006, 2008; Zhang et al., 2007, 2009; Kresse et al., 2013; Kear et al., 2017; Xu et al., 2019), distinct element method (DEM) (e.g. Yoon et al., 2014, 2015a, b; Zangeneh et al., 2015; Damjanac and Cundall, 2016; Zhang et al., 2018), and hybrid finite-distinct element method (FDEM) (e.g. Lisjak et al., 2017).

In this study, we aim to investigate the interactions between hydraulic and natural fractures in low permeability granitic rock using a numerical model developed in FRACOD2D (fracture propagation code), a two-dimensional (2D) boundary element code based on the DDM principles with integrated fracture mechanics approach (Shen et al., 2014). The added value of using FRACOD in this study is that it can simulate the explicit fracturing of brittle rocks. FRACOD has been used extensively for modelling of rock fracturing processes in numerous applications (e.g. Rinne et al., 2013; Shen, 2014; Shen et al., 2014, 2015; Barton and Shen, 2017), including coupled HM simulations of hydraulic fracturing (Shen and Shi, 2016; Xie et al., 2016; Janiszewski et al., 2018). Xie et al. (2016) presented a validation case of the hydraulic fracture simulator in FRACOD and demonstrated an example of the interaction between hydraulic and natural fractures. However, only one case with a low approach angle was tested. Hence, the first objective of this study is to test whether the realistic interaction mechanisms at different approach angles can be reproduced in FRACOD enhanced by the new fracture crossing function. The second objective is to validate the FRACOD model against the analytical criterion for fracture crossing by Sarmadivaleh and Rasouli (2014).

The structure of this paper is as follows. First, we introduce a brief summary of FRACOD theory and the new functionality of FRACOD that enables crossing of natural fractures by an approaching hydraulic fracture. Then, we test the new FRACOD improvement in a series of coupled HM models simulating an interaction between hydraulic and natural fractures in granitic rock for a range of approach angles. We discuss the implications of the fracture interaction on the HYDROCK method. Next, we validate the FRACOD model against an analytical criterion for fracture crossing. Finally, we investigate the evolution of the interaction mechanisms as a function of the controlling parameters.

2. Theoretical background of FRACOD

FRACOD uses an indirect boundary element technique – DDM for stress analysis, with fracture mechanics theory integrated into it. FRACOD is based on analytical solutions of displacements and stresses that are produced by a constant displacement discontinuity over a finite crack element in an infinite elastic body. The DDM method helps to find the discrete approximation of the smooth distribution of relative displacement presented in real cracks (Shen et al., 2014).

FRACOD uses the *F*-criterion for fracture propagation that was first proposed by Shen and Stephansson (1994) as a modified maximum strain energy release rate criterion (G-criterion). The F-criterion is capable of simulating mode I (tension) and mode II (shear) fracture propagation independently, along with mixed mode (mode I-II) fracture propagation taking place concurrently. The F-criterion is used to determine the propagation direction ϑ of the fracture and the failure load by calculating the sum of strain energy release rate for both mode I (G_I) and mode II (G_{II}), normalised by the critical strain energy release rates G_{IC} and G_{IIC}. Fracture propagation takes place when the following equation is satisfied:

$$F(\vartheta) = \frac{G_I(\vartheta)}{G_{IC}} + \frac{G_{II}(\vartheta)}{G_{IIC}} \geq 1 \tag{1}$$

Fracture initiation in the intact rock can take place in tension or shear. For mode I tensile fractures, one of the criteria that can be used is the tensile stress criterion, which predicts that fracture initiation will occur when the tensile stress is larger than or equal to the tensile strength of rock:

$$\sigma_t \geq T_0 \tag{2}$$

where σ_t is the tensile stress, and T_0 is the tensile strength of rock.

The other failure criterion that can be used for tensile fracture initiation is the extensional strain criterion (Barton and Shen, 2017). The generated mode I fracture is perpendicular to the maximum tensile stress (or extensional strain).

For mode II shear fractures, one of the criteria that can be used is the Mohr-Coulomb criterion, which predicts that fracture initiation will occur when the shear stress is larger than or equal to the shear strength of rock:

$$\sigma_s \geq \sigma_n \tan \varphi + c \tag{3}$$

where σ_s is the shear stress, σ_n is the normal stress, φ is the internal friction angle of intact rock, and c is the cohesion of intact rock.

Another shear criterion that can be used is the modified non-linear Mohr-Coulomb criterion (Shen et al., 2018). Mode II fractures are generated in the direction of the predicted shear failure plane.

FRACOD can simulate the bidirectional HM coupling using an explicit approach, where both the deformation with fracture propagation and the fluid flow are simulated using the time marching iteration scheme. The fluid flow in fractures is fully dynamic and governed by the cubic law. The use of cubic law and laminar flow is based on an assumption that the flow plane is narrow and the flow speed is relatively low, and hence the turbulent flow can be neglected. A more detailed description of the HM coupling in FRACOD, as well as a validation case of hydraulic fracturing simulator, was given by Xie et al. (2016).

As the hydraulic fracture is propagating horizontally, the fracture tips will reach the inclined pre-existing fracture and will lose the fracture tip. Hence the fracture criterion, i.e. the F-criterion, is no longer applicable. Therefore, new functionality is added to FRACOD to allow for the crossing of pre-existing fractures by the propagating hydraulic fracture. The FRACOD code is enhanced by checking the stress state at the surface of the fracture and then determining whether a fracture initiation is possible using the stress-based initiation criterion (i.e. the tensile stress criterion for tensile failure (Eq. (2)) and the Mohr-Coulomb criterion for shear failure (Eq. (3)). This new FRACOD functionality is tested and validated in the subsequent sections of this paper.

3. Modelling the interactions between hydraulic and natural fractures in FRACOD

3.1. Adaptive modelling approach

This study can be considered as a data-limited problem because no experimental data were produced, and the amount of information from the literature was limited. The rock mass is a highly non-uniform material, and thus the outcomes from one site may not apply to another location. Hence, the adaptive modelling approach suggested by Starfield and Cundall (1988) was employed to overcome the difficulties of a data-limited problem:

(1) The aim of modelling. The aim of modelling is to study the interaction between induced hydraulic fracture and pre-existing natural fracture that may arrest the induced fracture and inhibit its growth, which could lead to problems with permeability enhancement of the rock mass.
(2) Conceptual model. The model represents a 2D section of the rock mass characterised by high differential rock stress where $\sigma_{XX} > \sigma_{YY}$, with a single injection well generating the hydraulic fracture that is propagating horizontally, until it approaches and interacts with the natural fracture (see Fig. 2).
(3) Mechanics of the problem. The induced hydraulic fracture may interact with the natural fracture that lies on its propagation path and five types of geomechanical interaction mechanisms are possible, i.e. crossing, arresting (no crossing), dilation, activation, and offset crossing. Additionally, mixed mechanisms are also possible. The development of those mechanisms is depicted in Fig. 3. A more comprehensive description of the possible interactions was given by Cheng et al. (2015).
(4) Experiment. The approach angle was varied to test if the realistic interaction mechanisms described in the previous steps can be reproduced numerically. Results are compared to analytical criteria from the literature and discussed in relation to HYDROCK method.
(5) Increasing complexity. Once the simple model has been explored and the lessons are learned, the complexity can be increased in order to study other aspects of geology that have been omitted, for example, more extensive fracture network consisting of one or more joint sets. However, this study only considered a single hydraulic fracture interacting with a natural fracture.

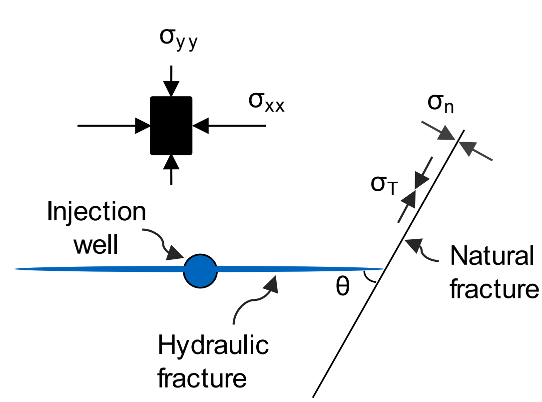

Fig. 2. A conceptual model of an interaction between hydraulic and natural fractures inclined at an approach angle θ in relation to an induced hydraulic fracture in high differential in situ rock stress conditions where $\sigma_{XX} > \sigma_{YY}$.

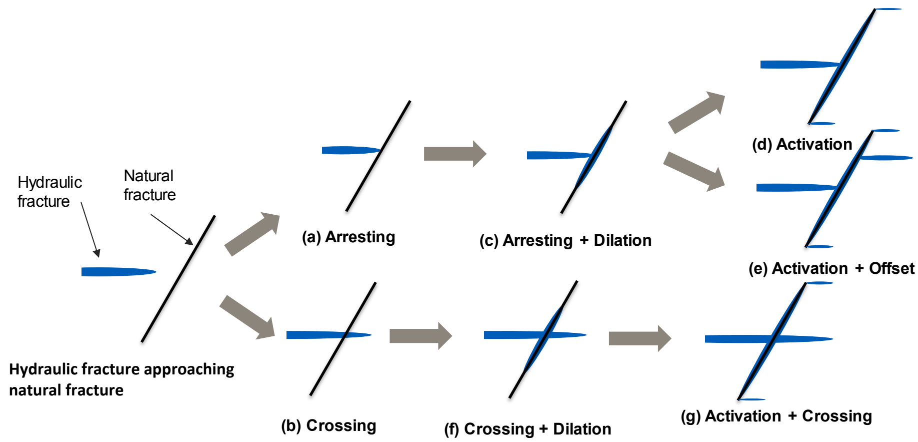

Fig. 3. Schematic representation of possible interactions between hydraulic and natural fractures. (a) First, if the induced tensile stress at the hydraulic fracture tip is larger than the tensile strength behind the natural fracture and no shear displacement takes places along the natural fracture, the hydraulic fracture will cross the natural fracture. (b) If the two conditions are not met, the hydraulic fracture will become arrested at the natural fracture. (c, f) The fluid front will reach the natural fracture and may dilate it if the water pressure exceeds the normal stress acting on the fracture surface. This will create a bifurcation of the flow into the natural fracture. (d, g) The natural fracture may be activated either due to shear slippage or fluid penetration that may cause further fracture initiation and propagation from the natural fracture tips, which will result in fracture branching. (e) An offset crossing may occur due to stress concentrations along the fracture, which will cause further branching of the fracture. Redrawn from Cheng et al. (2015).

3.2. Model setup in FRACOD

The numerical model was developed in FRACOD according to the conceptual model given in Fig. 2. The 2D model consisted of an injection well of 0.1 m diameter with a pre-existing fracture extending from the borehole as a kink for simplifying fracture propagation. A natural fracture of 0.3 m in length was placed to the right of the borehole at a distance of 0.2 m. The model was symmetrical against the central point ($X = 0$ m, $Y = 0$ m). A grid size of 0.01 m was used. A series of models was prepared with the approach angle θ ranging between 90° and 40° at 10° interval. An example of the model geometry with the approach angle equal to 60° is shown in Fig. 4. It has to be noted that the model represented a vertical section of the rock mass with the source of fluid pressure modelled as a circle. Also, the geometry of 0.5 m × 0.5 m was only used for plotting the results, and the actual model geometry extended infinitely according to the principles of the BEM where only the inner boundary problem was simulated.

To simulate hydraulic fracturing, a synthetic granitic rock mass was assumed that reflects the realistic geomechanical properties of the Bohus granite, which hosted the first HYDROCK field experiment conducted by Larson et al. (1983). The input properties used for the numerical model are given in Table 1. The assumed values aimed to reflect the typical properties of granitic rock. The far-field in situ rock stresses were assumed to be 8 MPa and 1.5 MPa in the horizontal and vertical directions, respectively.

The tensile stress criterion (Eq. (2)) was used for tensile fracture initiation and the Mohr-Coulomb failure criterion (Eq. (3)) for shear fracture initiation, which allows fracture initiation at fracture surfaces to fracture crossing. The fluid flow was fully dynamic with a constant injection pressure of 8 MPa assigned to the borehole boundary. Water at a temperature of 20 °C with a bulk modulus of 2 GPa and a dynamic viscosity of 0.001 Pa s was used as the fracturing fluid in the simulation.

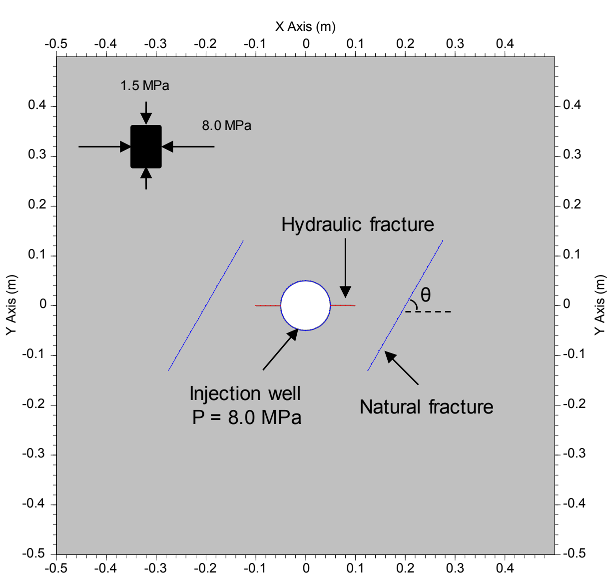

Fig. 4. Example of the model geometry in FRACOD for approach angle equal to 60°.

4. Results of the interactions for a series of approach angles

The modelling results of the interactions between hydraulic and natural fractures are shown in Figs. 5 and 6. It can be observed that the interactions between hydraulic and natural fractures are dependent on the approach angle.

The models containing natural fracture at large approach angles ($\theta \geq 70°$) (Fig. 5a–c) simulated the crossing interaction mechanism as shown in Fig. 3b. The natural fracture was also dilated and sheared in the vicinity of the intersection point due to induced stresses ahead of the hydraulic fracture tip (dilation). Nevertheless, the fracturing fluid did not penetrate the natural fracture within the given time period and only followed the path of the propagating hydraulic fracture that crossed the natural fracture (Fig. 6a). This can be explained by the very low aperture of the natural fracture (1 μm) and high horizontal stress resulting in high normal stresses acting on the natural fracture surface, which prevented complete opening of the natural fracture and the fluid pressure build-up in the tight fracture. The induced fracture was hydraulically conductive (Fig. 6d) and hence, the presence of natural fracture situated at large angles with respect to the hydraulic fracture appears not to impair the construction process of the HYDROCK method.

Table 1
Input parameters for the numerical model that reflect a granitic rock mass of low permeability.

Input parameter	Value	Source
Rock type	Bohus granite	Larsson (1983)
Intact rock tensile strength, σ_t (MPa)	10.5	
Intact rock friction angle, φ (°)	45	Assumed
Intact rock cohesion, c (MPa)	25	
Elastic modulus, E (GPa)	53	Larsson (1983)
Poisson's ratio, ν	0.2	
Mode I fracture toughness, K_{IC} (MPa m$^{1/2}$)	1.8	Liu et al. (2010)
Mode II fracture toughness, K_{IIC} (MPa m$^{1/2}$)	4	Assumed
Horizontal in situ stress, σ_{XX} (MPa)	−8	Larsson (1983)
Vertical in situ stress, σ_{YY} (MPa)	−1.5	
Fracture shear stiffness, k_s (GPa/m)	3099	Shen et al. (2011)
Fracture normal stiffness, k_n (GPa/m)	13,800	
Fracture friction angle, φ_f (°)	45	From intact rock strength
Fracture cohesion, c_f (MPa)	0	Assumed
Fracture dilation angle, φ_d (°)	0	
In situ hydraulic conductivity, K_{is} (m/s)	1×10^{-19}	
Fracture initial aperture, $e_{initial}$ (μm)	1	
Fracture residual aperture, e_{resid} (μm)	1	
Fluid injection pressure, P_{in} (MPa)	8	
Fluid bulk modulus, E_w (GPa)	2	
Fluid viscosity, μ (Pa s)	0.001	
Fluid density, ρ (kg/m^3)	1000	

At an approach angle equal to 60° (Figs. 5d and 6b), the model reproduced the activation and offset crossing interaction mechanism as shown in Fig. 3e. Due to the lower normal stress acting on the natural fracture surface, the natural fracture experienced shear displacement that caused its activation and mode I fracture initiation from its upper tip in the direction of the maximum horizontal stress. In addition, the shear movement of the natural fracture resulted in stress concentration and offset crossing of the hydraulic fracture.

The models containing the natural fracture at low approach angles ($\theta \le 50°$) (Fig. 5e and f) simulated the arresting and activation of hydraulic and natural fracture interaction as shown in Fig. 3d. The slippage of the natural fracture resulted in mode I fracture initiated at the upper tip of the natural fracture that propagated into the rock mass as a dry wing-shaped fracture (Fig. 5f). Then, the fracturing fluid penetrated the newly formed tensile fracture and propagated it further in the direction of the maximum horizontal stress (Fig. 6c). This type of wing-shaped fracture is identical to wing-fractures generated in the laboratory by loading rock specimens with inclined fracture (Shen et al., 1995). This outcome agrees well with the results of PFC2D numerical simulations of hydraulic and natural fracture interactions by Yoon et al. (2017) and Zhang et al. (2018) who observed similar fractures in their numerical models. Arresting, activation and propagation of the wing-shaped tensile fractures result in a more complex fracture propagation path, which differs from the ideal sub-horizontal fracture that was assumed in the ideal HYDROCK case described by Hellström and Larson (2001). Even though the

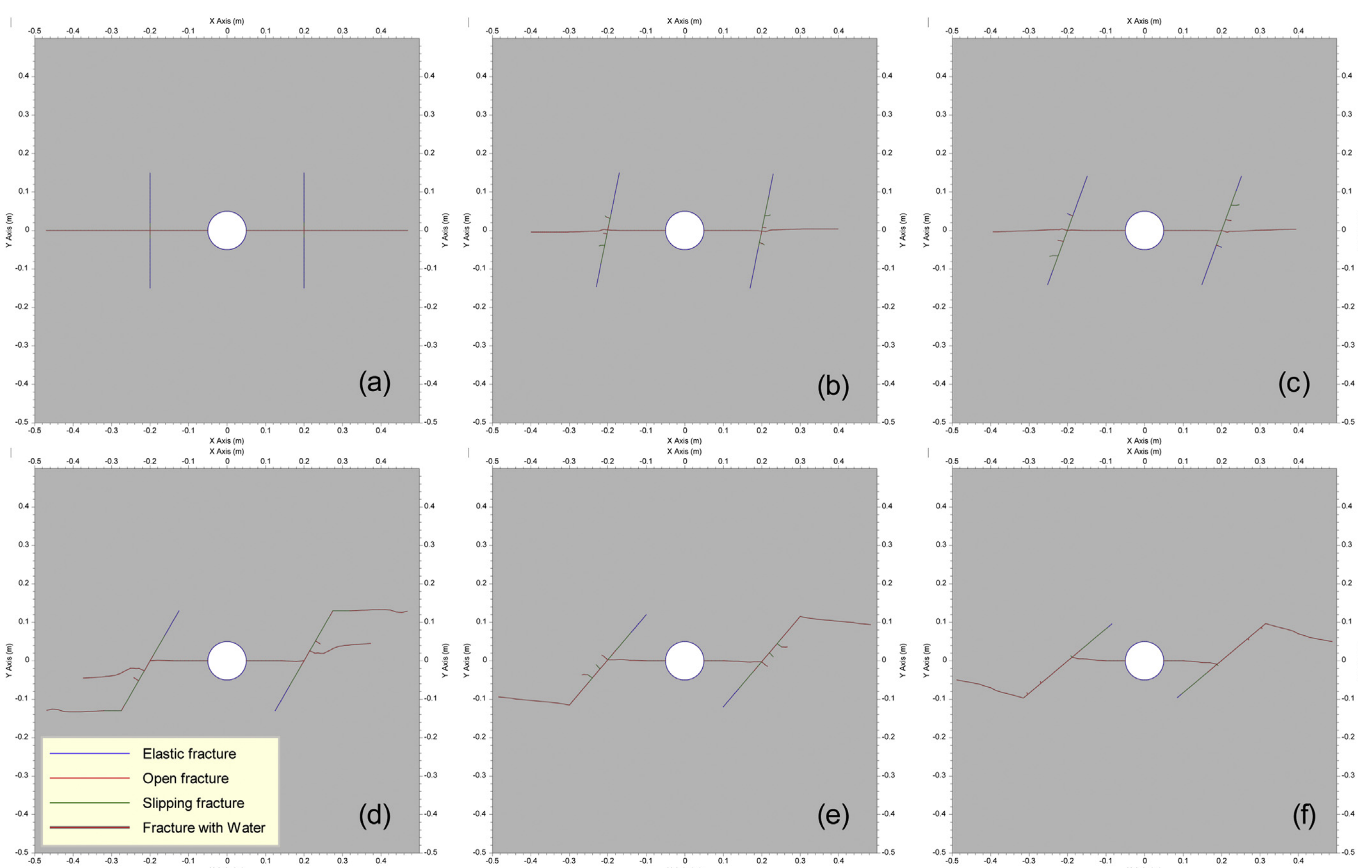

Fig. 5. FRACOD modelling results of the interactions with a natural fracture. (a–c) At approach angles $\theta = 90°$, 80°, and 70°, the hydraulic fracture crossed the natural fracture and propagated further into the rock mass; (d) At $\theta = 60°$, the hydraulic fracture crossed the natural fracture at an offset and activated the natural fracture due to shear slippage causing propagation from the tip of the natural fracture; (e, f) At $\theta = 50°$ and 40°, the hydraulic fracture was arrested at the natural fracture, causing its activation and opening by the penetrating fluid that resulted in further propagation from the upper tip of the natural fracture.

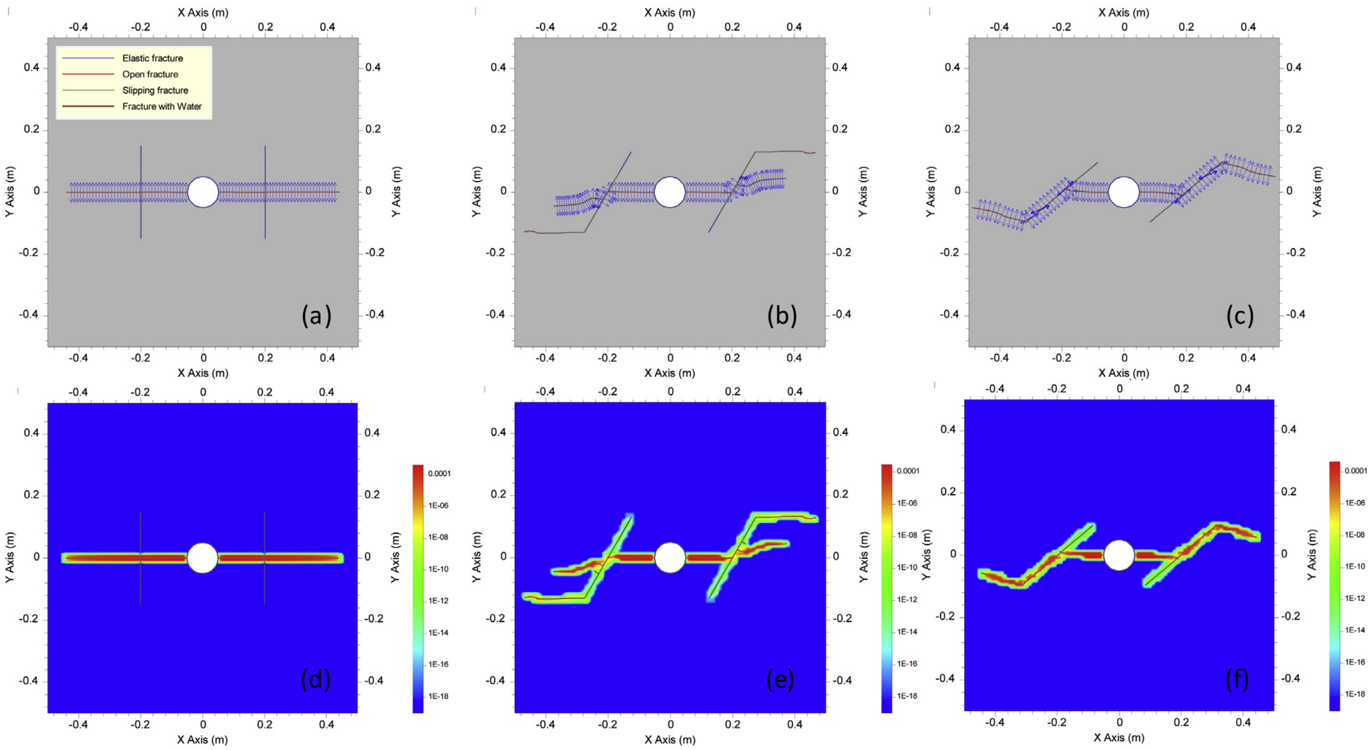

Fig. 6. Modelling results depicting fluid pressure distribution (a–c) and hydraulic conductivity (d–f) for three different interaction mechanisms of the hydraulic and natural fractures: (a–c) Fluid pressure distribution within the fractures for approach angles $\theta = 90°$, 60°, and 40°, respectively; and (d–f) Hydraulic conductivity of fractures for approach angles $\theta = 90°$, 60°, and 40°, respectively.

fractures are hydraulically conductive (Fig. 6e and f), coalescence of multiple fracture planes could occur at different depths that would reduce the total heat exchange area, decreasing the thermal performance of the HYDROCK method.

The obtained results of the dependency of the interaction between hydraulic and natural fractures on the approach angle are in good agreement with previous experimental (e.g. Zhou et al., 2008; Cheng et al., 2014) and numerical studies (e.g. Yoon et al., 2017; Zhang et al., 2018). FRACOD is able to simulate all interaction mechanisms, such as crossing, arresting, dilation, activation, and offset crossing, which were described by Cheng et al. (2015).

Nevertheless, some differences were observed in the branching of the fractures from the tip of the natural fracture compared to the schematic representation of interaction mechanisms depicted in Fig. 3d, e and g. Due to the displacement of the block below the right wing of the hydraulic fracture (Fig. 7a), the bottom half of the natural fracture is closed, resulting in very low aperture (Fig. 7b), so that the fluid can only penetrate the upper part of the natural fracture (Fig. 7c). An analogous result was obtained by Xie et al. (2016), where no bifurcation of the flow was observed in FRACOD model of hydraulic and natural fracture interaction, even though the natural fracture had an initial aperture of 100 μm. However, no fracture crossing function was used in their study and only one approach angle was tested. This behaviour can differ if the initial aperture of the natural fracture is larger, as the used value of 1 μm represents a very low permeability fracture. Higher fracture

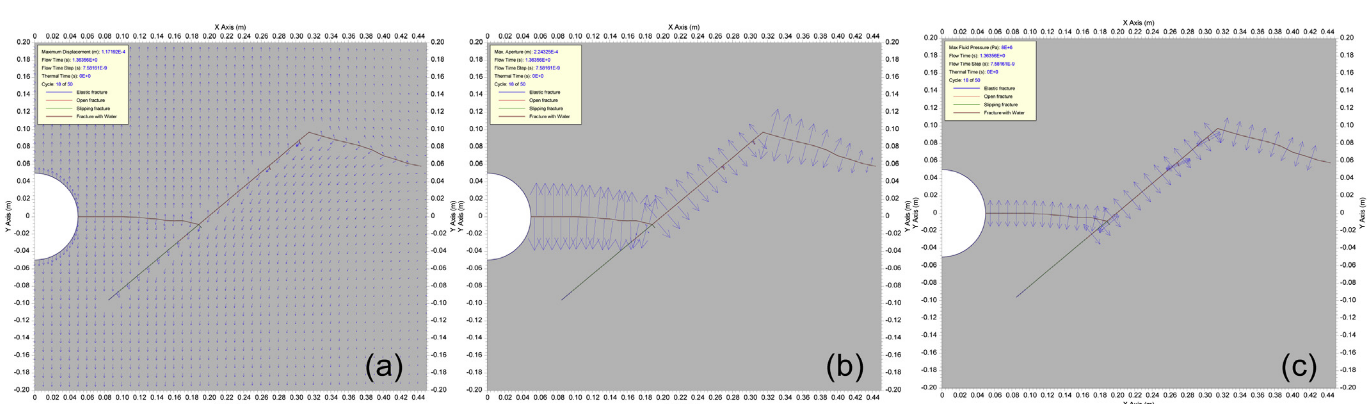

Fig. 7. Close-up view of simulated interaction from Fig. 5f at approach angle equal to 40°: (a) Displacement distribution, (b) Fracture aperture, and (c) Fluid pressure distribution. Due to the displacement of the block below the right wing of the hydraulic fracture (a), the bottom half of the natural fracture is closed, resulting in very low aperture (b), so that the fluid can only penetrate the upper part of the natural fracture (c).

Table 2
Comparison of numerical predictions in FRACOD and modified Renshaw and Pollard analytical criterion by Sarmadivaleh and Rasouli (2014).

θ (°)	σ_{XX} (MPa)	σ_{YY} (MPa)	σ_n (MPa) (Eq. (6))	σ_T (MPa) (Eq. (7))	τ (MPa) (Eq. (10))	τ_0 (MPa) (Eq. (9))	μ_f	Analytical (Eq. (4))	FRACOD
90	−8	−1.5	−8	−1.5	0	8	1	Crossing	Crossing
80	−8	−1.5	−7.8	−1.7	1.1	7.8	1	Crossing	Crossing
70	−8	−1.5	−7.2	−2.3	2.1	7.2	1	Crossing	Crossing
60	−8	−1.5	−6.4	−3.1	2.8	6.4	1	Crossing	Activation + offset crossing
50	−8	−1.5	−5.3	−4.2	3.2	5.3	1	Arresting	Arresting + activation
40	−8	−1.5	−4.2	−5.3	2.8	4.2	1	Arresting	Arresting + activation

aperture could allow the fluid to penetrate and dilate the natural fracture, resulting in the bifurcation of the flow. This problem is addressed in Section 5, where the interactions of hydraulic fracture with a pre-existing natural fracture of larger aperture are tested.

It also has to be noted that the results presented in this study are limited to a 2D case of the hydraulic and natural fracture interaction, e.g. the horizontal hydraulic fracture interacting with the dipping natural fracture, which neglects the influence of the natural fracture strike angle. A criterion that addresses this problem in three-dimensional (3D) space was given by Cheng et al. (2014), which states that crossing can take place only at large approach and strike angles. In addition, the fracture propagation and release of the hydraulic pressure in 3D space will tend to follow the path of least resistance and can propagate also in the out-of-plane direction, where there is no discontinuity that disturbs the stress field ahead of the fracture tip. Therefore, it is recommended to study this problem in future using a numerical code that is capable of coupled HM simulations in 3D space.

Results of the simulations were compared to the modified Renshaw and Pollard analytical criterion for a non-orthogonal natural interface intersected by an induced fracture developed by Sarmadivaleh and Rasouli (2014). The criterion predicts whether the induced fracture will cross the interface or become arrested at the interface. The crossing occurs when the following equation is satisfied (Sarmadivaleh and Rasouli, 2014):

$$\frac{-\sigma_n}{T_0-\sigma_T} > \frac{\left(1-\sin\frac{\theta}{2}\sin\frac{3\theta}{2}\right)+\left|\sin\frac{\theta}{2}\cos\frac{\theta}{2}\cos\frac{3\theta}{2}+\alpha\right| \Big/ \left(\mu''_f\cos\frac{\theta}{2}\right)}{1+\sin\frac{\theta}{2}\sin\frac{3\theta}{2}} \tag{4}$$

where μ''_f is an imaginary friction coefficient, σ_T is the tangential stress applied on the natural fracture surface (Jaeger et al., 2007), and α is a coefficient. These parameters can be calculated as follows:

$$\mu''_f=\mu_f+\mu'_f=\mu_f+\frac{\tau_0/\sigma_n}{\dfrac{1-\sin\frac{\theta}{2}\sin\frac{3\theta}{2}}{\left(1-\sin\frac{\theta}{2}\sin\frac{3\theta}{2}\right)+\left|\sin\frac{\theta}{2}\cos\frac{\theta}{2}\cos\frac{3\theta}{2}+\alpha\right| \Big/ \left(\mu_f\cos\frac{\theta}{2}\right)}-1} \tag{5}$$

$$\sigma_n=\frac{\sigma_{XX}+\sigma_{YY}}{2}+\frac{\sigma_{XX}-\sigma_{YY}}{2}\cos(\pi-2\theta) \tag{6}$$

$$\sigma_T=\frac{\sigma_{XX}+\sigma_{YY}}{2}-\frac{\sigma_{XX}-\sigma_{YY}}{2}\cos(\pi-2\theta) \tag{7}$$

$$\alpha=\frac{\tau}{\frac{T_0-\sigma_T}{\cos(\theta/2)[1+\sin(\theta/2)\sin(3\theta/2)]}} \tag{8}$$

$$\tau_0=\sigma_n\tan\varphi_f+c_f \tag{9}$$

$$\tau=\frac{\sigma_{XX}-\sigma_{YY}}{2}\sin(\pi-2\theta) \tag{10}$$

where τ is the shear stress applied along the natural fracture (Jaeger et al., 2007), τ_0 is the Mohr-Coulomb joint shear strength, and μ_f is the friction coefficient.

The results of the comparison are shown in Table 2. It can be observed that FRACOD predicts the same type of interaction as the analytical criterion does. Only in one case – when the approach angle is equal to 60°, the FRACOD model simulates activation and offset crossing, whereas the analytical criterion predicts crossing. However, it should be noted that the analytical criterion can only predict whether the hydraulic fracture will cross the natural fracture and cannot predict any complex interactions, such as the mixed activation and offset crossing mode. Hence, it can be concluded that the numerical predictions obtained from FRACOD agree with the analytical predictions.

5. Investigation of the evolution of the interaction mechanisms as a function of controlling parameters

Several scenarios were prepared to test the influence of other controlling parameters on the evolution of the interaction mechanisms between the propagating hydraulic fracture and the pre-existing natural fracture.

5.1. The effect of fracture aperture

The fracture aperture dictates its permeability so that a larger aperture results in an easier penetration of the fracturing fluid. To test the effect of the natural fracture's aperture on the crossing behaviour, the pre-existing fracture's aperture was varied between 1 μm, 10 μm, 25 μm and 50 μm, respectively. The dip angles of the natural fracture equal to 90°, 60° and 40° were used to reproduce multiple interaction mechanisms. All parameters were set the same as those in Table 1. The modelling results are given in Fig. 8. It can be seen that in models with the natural fracture dipping at 90° (Fig. 8a–d), the larger the aperture is, the easier the fracturing fluid penetrates and opens the fracture. However, increasing the aperture did not change the fracturing pattern, because the natural fracture's tips were not activated and the hydraulic fracture simply crossed the natural fracture with the same propagation path. In models with the natural fracture dipping at 60° (Fig. 8e–h), the interaction mechanisms changed with the increased fracture aperture. When the aperture was equal to 1 μm (Fig. 8e), the hydraulic fracture crossed the natural fracture at a small offset because the fluid could not penetrate the natural fracture. As the aperture increased (Fig. 8f and g), the fluid penetrated the natural fracture and then crossed the natural fracture at a point located further away from the intersection when compared to the previous

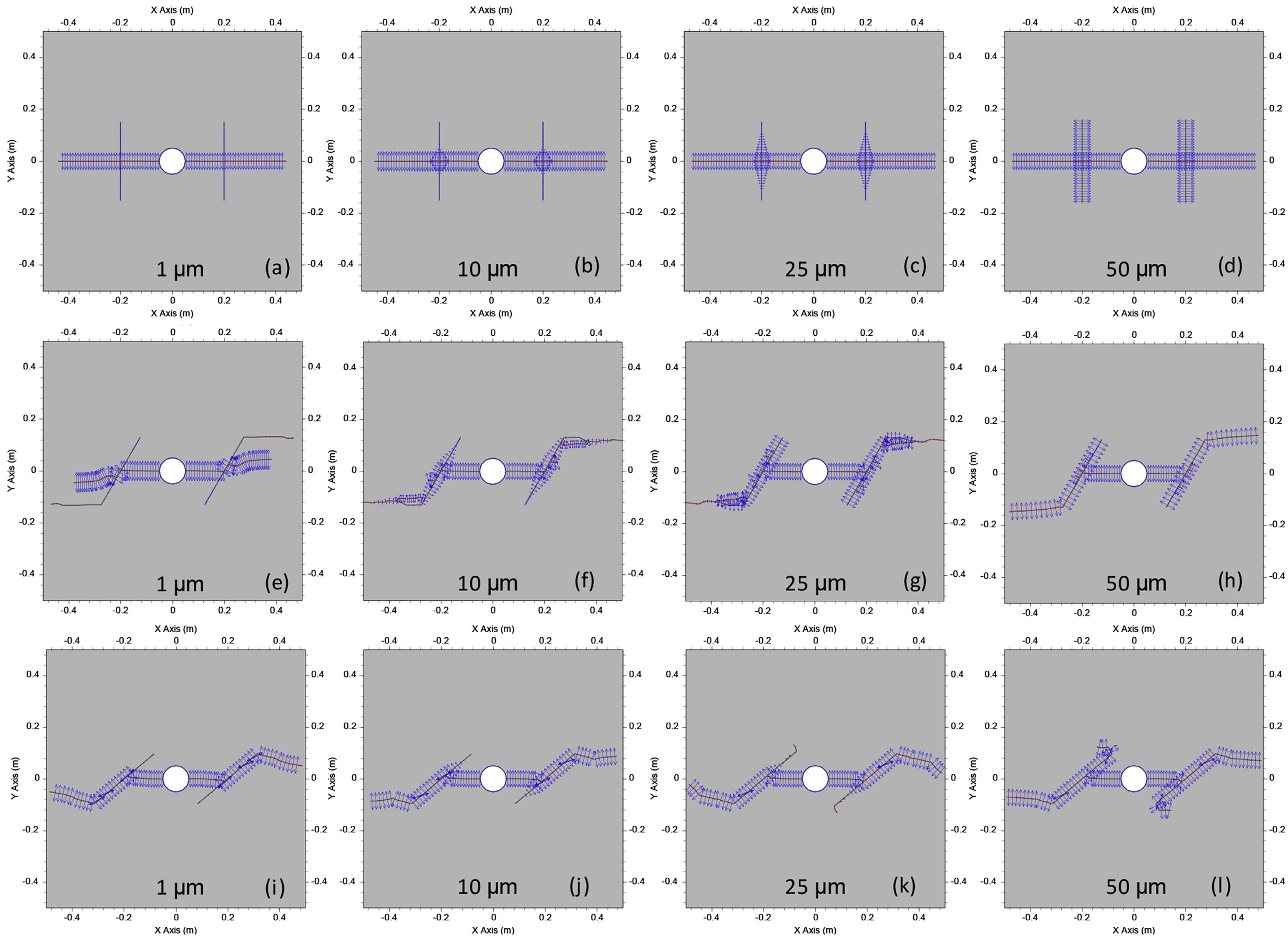

Fig. 8. Modelling results depicting fracturing pattern and fluid pressure distribution as a function of the natural fracture's aperture equal to 1 μm, 10 μm, 25 μm and 50 μm, respectively: (a–d) Approach angle $\theta = 90^\circ$, (e–h) $\theta = 60^\circ$, and (i–l) $\theta = 40^\circ$. A general observation is that the larger the fracture aperture, the easier the fracturing fluid infiltrates the pre-existing fracture and changes the interaction mechanism.

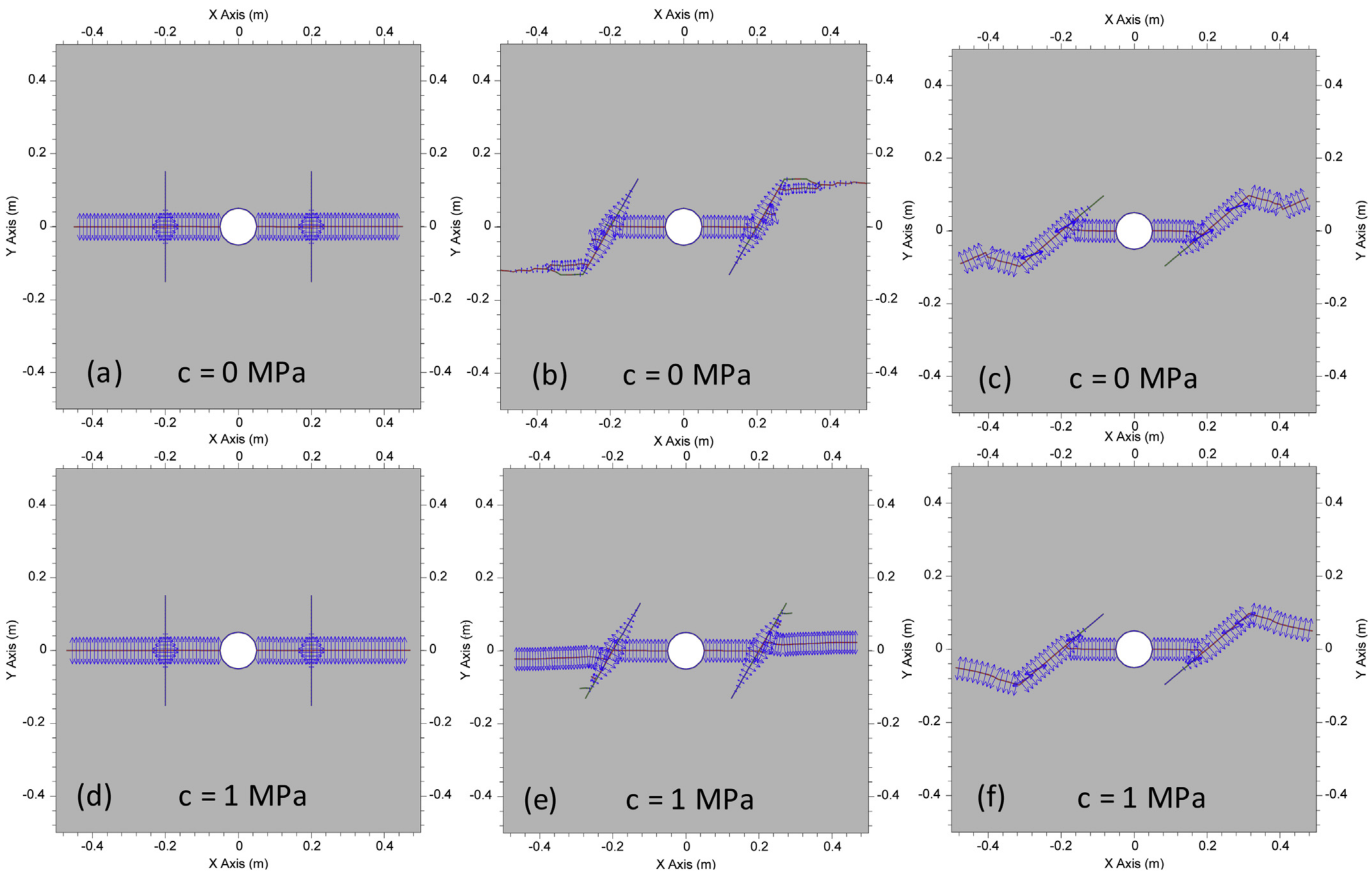

Fig. 9. Modelling results depicting fracturing pattern and fluid pressure distribution as a function of the natural fracture's cohesion: (a–c) No cohesion, and (d–f) Cohesion equal to 1 MPa, for approach angles equal to 90°, 60°, and 40°, respectively. The increased shear strength of the pre-existing fracture dipping at 40° changes the interaction mechanism to crossing (e) in comparison to the activation and offset crossing interaction mechanism in the cohesionless case (b).

case. At the same time, the upper tip of the natural fracture was activated and mode I fracture initiation occurred in the direction of maximum horizontal stress. The hydraulic fracture ultimately coalesced with this fracture creating a similar fracture pattern as arresting and activation type of hydraulic and natural fracture interaction mechanism shown in Fig. 3d. In models with the approach angle of 40° (Fig. 8i–l), the increase of fracture aperture did not change the arresting and activation interaction mechanism. However, the larger the aperture, the easier the fluid permeates the natural fracture, resulting in the bifurcation of the flow and branching of the hydraulic fracture from both tips of the natural fracture (Fig. 8l).

5.2. The effect of fracture cohesion

The effect of increased shear strength of the pre-existing fracture was tested by setting the cohesion of the natural fracture to 1 MPa (Fig. 9d–f) and comparing it with the cohesionless case where fracture cohesion was 0 MPa (Fig. 9a–c). All parameters were set the same as those in Table 1, except the aperture of the natural fracture, which was set to 10 μm.

Here, the difference was most visible in the scenario with approach angle of 60°, where the increased shear strength of the natural fracture promoted the crossing interaction mechanism (Fig. 9e) compared to the arresting and offset crossing interaction mechanism in the cohesionless case (Fig. 9b). In the model with natural fracture dipping at 40° (Fig. 9c and f), the only difference was a slight change of the path of the wing-shaped mode I fracture that propagated from the tip of the natural fracture. These results are in line with the observations in the literature, for example, PFC2D models made by Zhang et al. (2018).

5.3. The effect of differential in situ rock stress

The differential in situ rock stress is one of the factors in the analytical criteria for fracture crossing prediction (e.g., Sarmadivaleh and Rasouli, 2014). To test the interactions of hydraulic and natural fractures in a less anisotropic in situ rock stress environment in FRACOD, the vertical in situ rock stresses was increased to 4 MPa (Fig. 10d–f) while keeping the horizontal stress at 8 MPa. All other parameters were set the same as those in Table 1, except the aperture of the natural fracture that was set to 10 μm. The injection pressure in the models with the lower differential stress was increased to 14.5 MPa to enable propagation of the hydraulic fracture. The modelling results are depicted in Fig. 10.

The difference in the interaction behaviour is most visible in the scenario with the approach angle of 60° (Fig. 10e), which resulted in the crossing interaction mechanism, as opposed to the model with more anisotropic in situ rock stresses that resulted in activation and offset crossing interaction mechanism (Fig. 10b). The difference can be attributed to the higher value of vertical stress, which resulted in greater normal stress acting on the natural fracture. Hence the crossing was more plausible and the propagation path was different.

5.4. The effect of fluid viscosity

Ishida et al. (2004) and Chen et al. (2015) observed in laboratory experiments of hydraulic fracturing in granitic specimens that

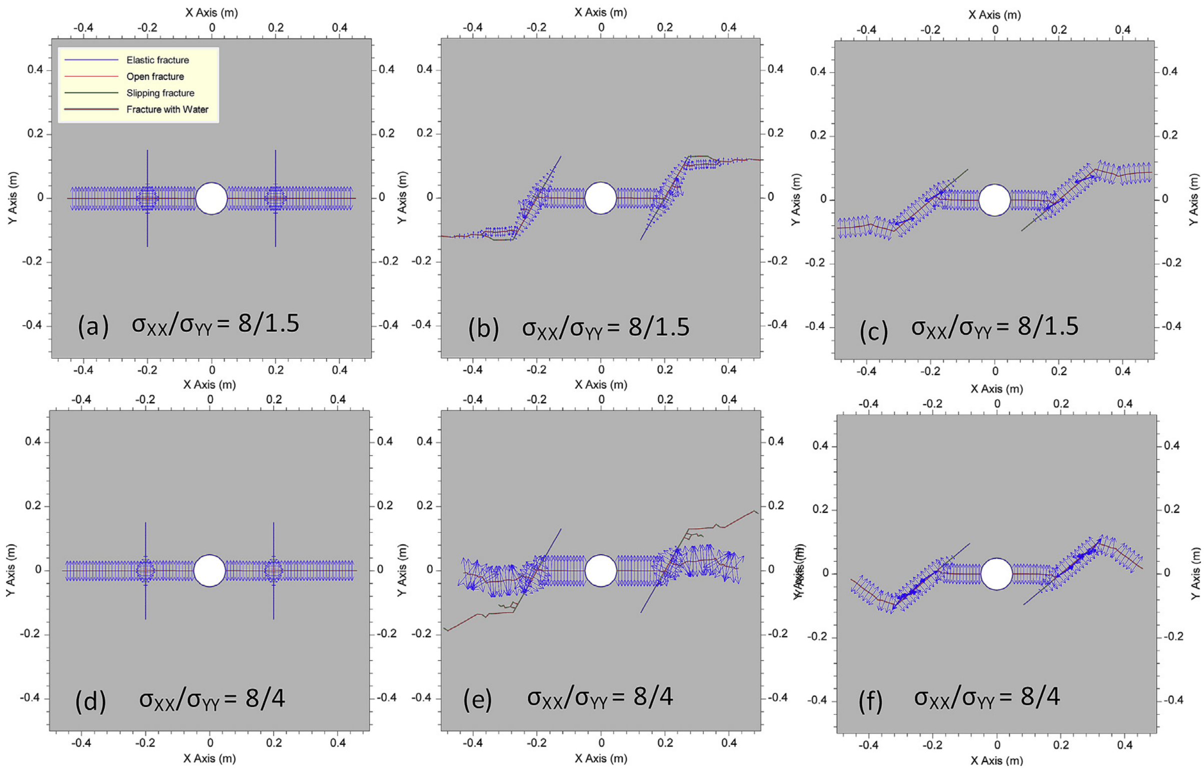

Fig. 10. Modelling results depicting fracturing pattern and fluid pressure distribution as a function of the in situ rock stresses acting in *X* and *Y* directions: (a–c) Horizontal stress $\sigma_{XX} = 8$ MPa and vertical stress $\sigma_{YY} = 1.5$ MPa, (d–f) $\sigma_{XX} = 8$ MPa and $\sigma_{YY} = 0.5$ MPa, and (g–i) $\sigma_{XX} = 8$ MPa and $\sigma_{YY} = 4$ MPa, for approach angles $\theta = 90^\circ$, 60°, and 40°, respectively.

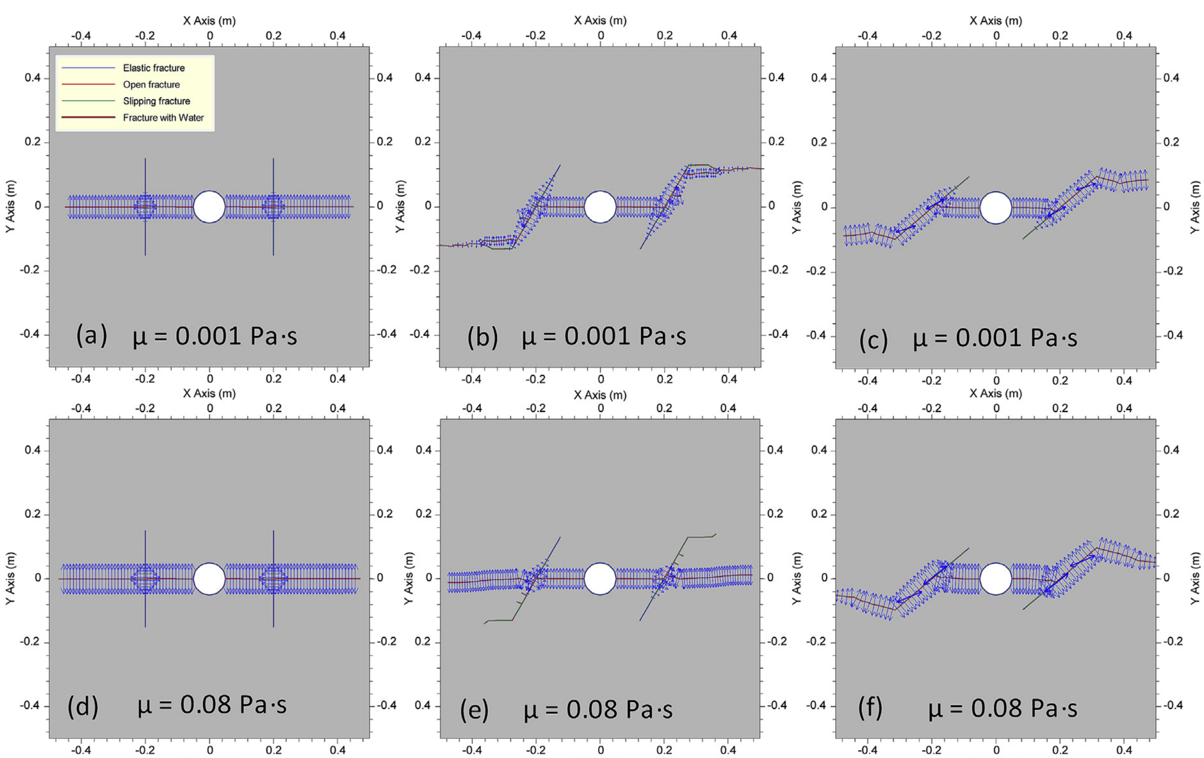

Fig. 11. Modelling results depicting fracturing pattern and fluid pressure distribution as a function of fluid viscosity: (a–c) Low viscosity, and (d–f) High viscosity, for approach angles $\theta = 90^\circ$, 60°, and 40°, respectively. The fractures that propagated with high viscosity oil are less convoluted compared to the fractures propagating with water. At approach angle equal to 60°, fluid viscosity has an influence on the type of interaction between the hydraulic and natural fractures.

modifying the fracturing fluid viscosity influences the pattern of fracture propagation path so that a lower viscosity fracturing fluid creates a more convoluted fracture network with more branching. To test the influence of fluid viscosity on the interactions between hydraulic and natural fractures in FRACOD, the fluid viscosity of the fracturing fluid was set to 0.001 Pa s and 0.08 Pa s, which correspond to water and oil used by Ishida et al. (2004), respectively. All other parameters were set the same as those in Table 1, except the aperture of the natural fracture that was set to 10 μm. The modelling results are given in Fig. 11.

The difference between the hydraulic and natural fracture interaction with low and high viscosity fracturing fluids was most pronounced in the model with approach angle of 60°. Fracturing with water resulted in the arresting and offset crossing type of interaction mechanism and a more convoluted fracturing pattern (Fig. 11b). The hydraulic fracture crossed the natural fracture at an offset that later coalesced with the dry wing-shaped fracture that propagated from the natural fracture tip. In contrast, fracture with viscous oil resulted in the crossing type of interaction with a planar crack propagating directly across the natural fracture in the direction of horizontal stress (Fig. 11e). The results may be explained by the lower velocity of the high viscosity fluid that enabled faster pressure build-up required for crossing and created a more planar fracture. This result is consistent with laboratory observations by Ishida et al. (2004) and Chen et al. (2015) who also observed that high viscosity fracturing fluid creates more planar and smooth fractures. At approach angle equal to 40° (Fig. 11c and f), the same type of hydraulic and natural fracture interaction was observed. Even though the hydraulic fracture that propagated from the tip of the natural fracture with high viscosity fluid appeared as more planar (Fig. 11f), the differences were less pronounced. At approach angle equal to 90° (Fig. 11a and d), no differences were observed.

6. Conclusions

In this study, we briefly describe the new functionality of the fracture propagation code FRACOD that allows for fracture initiation from the fracture surface when a hydraulically driven fracture intersects a pre-existing natural fracture. We developed a series of coupled HM numerical models to simulate the interaction between hydraulic and natural fractures to study their implications on an artificially fractured hard rock aquifer for thermal energy storage. Based on the simulation results, the following conclusions are drawn:

(1) FRACOD, enhanced by the new crossing fracture functionality, can simulate all the interactions between induced hydraulic and natural fractures, including crossing, arresting, dilation, activation and offset crossing, as well as their combination. At large approach angles, the hydraulic fracture can cross the natural fracture and propagate further into the rock mass without changing the original propagation path. At small approach angles, the interactions between hydraulic and natural fractures involve arresting of the hydraulic fracture at the pre-existing fracture, its activation and development of wing-shaped tensile fracture from the tip of the natural fracture.
(2) The comparison of the numerical results and the modified Renshaw and Pollard analytical criterion for fracture crossing shows a general agreement for a series of approach angles.
(3) The presence of natural fractures that are inclined at large angles with respect to the horizontal hydraulic fracture does not prevent the development of sub-horizontal fracture planes for the HYDROCK method. Conversely, the presence of fractures inclined at low angles with respect to the horizontal hydraulic fracture can lead to fracture arrest and development of more complex fracture network. This may impair the thermal performance of the HYDROCK method due to the coalescence of multiple hydraulic fractures and a reduction of heat exchange area.
(4) An increase of the aperture of the natural fracture does have an influence on the interaction mechanism due to higher permeability of the pre-existing fracture that can lead to double branching of the flow in the arrest and activation interaction mechanism, or shifting the offset location in the activation and offset crossing mechanism.
(5) An increase of the natural fracture's cohesion is likely to promote the crossing type of interaction mechanism at intermediate approach angles due to an increase of the shear strength of the natural fracture that prevents its opening by the fracturing fluid and its activation.
(6) The interaction of hydraulic and natural fractures is dependent on the anisotropy of the in situ rock stresses and crossing of the natural fracture is more likely at intermediate approach angles with lower differential stress.
(7) The fluid viscosity has an influence on the type of interactions between hydraulic and natural fractures at intermediate approach angles. The use of low viscosity fracturing fluid, such as water, results in more convoluted fracturing pattern that can be beneficial for creating a larger heat exchange area in the HYDROCK method.

In future, numerical simulations based on the fracture mechanics approach will be used to study the interactions of single and multiple hydraulic fractures in a fractured rock mass that contains one or more joint sets to study their influence on HYDROCK method at the field scale.

Conflicts of interest

The authors wish to confirm that there are no known conflicts of interest associated with this publication and there has been no significant financial support for this work that could have influenced its outcome.

Acknowledgement

The financial support from Aalto Doctoral Programme in Engineering and the International Collaboration Project on Coupled Fracture Mechanics Modelling – Phase 3 (project team consisting of CSIRO, SDUST, Posiva, KIGAM, KICT, CAS-IRSM, DUT/Mechsoft, SNU, LBNL, ETH, Aalto Uni., GFZ and TYUT) is kindly acknowledged.

References

Amadei B, Stephansson O. Rock stress and its measurement. Dordrecht, the Netherlands: Springer; 1997.
Barton N, Shen B. Risk of shear failure and extensional failure around over-stressed excavations in brittle rock. Journal of Rock Mechanics and Geotechnical Engineering 2017;9(2):210–25.
Blanton TL. An experimental study of interaction between hydraulically induced and pre-existing fractures. In: SPE unconventional gas recovery symposium. Society of Petroleum Engineers (SPE); 1982. https://doi.org/10.2118/10847-MS.
Blanton TL. Propagation of hydraulically and dynamically induced fractures in naturally fractured reservoirs. In: SPE unconventional gas technology symposium. SPE; 1986. https://doi.org/10.2118/15261-MS.

Chen Y, Nagaya Y, Ishida T. Observations of fractures induced by hydraulic fracturing in anisotropic granite. Rock Mechanics and Rock Engineering 2015;48(4):1455–61.

Cheng W, Jin Y, Chen M, Xu T, Zhang Y, Diao C. A criterion for identifying hydraulic fractures crossing natural fractures in 3D space. Petroleum Exploration and Development 2014;41(3):371–6.

Cheng W, Jin Y, Chen M. Experimental study of step-displacement hydraulic fracturing on naturally fractured shale outcrops. Journal of Geophysics and Engineering 2015;12(4):714–23.

Clark JB. A hydraulic process for increasing the productivity of wells. Journal of Petroleum Technology 1949;1(1):1–8.

Cobbing J, Dochartaigh BÉÓ. Hydrofracturing water boreholes in hard rock aquifers in Scotland. Quarterly Journal of Engineering Geology and Hydrogeology 2007;40(2):181–6.

Dahi-Taleghani A. Analysis of hydraulic fracture propagation in fractured reservoirs: an improved model for the interaction between induced and natural fractures (PhD Thesis). Austin, USA: University of Texas; 2009.

Damjanac B, Cundall P. Application of distinct element methods to simulation of hydraulic fracturing in naturally fractured reservoirs. Computers and Geotechnics 2016;71:283–94.

Dehghan AN, Goshtasbi K, Ahangari K, Jin Y. Experimental investigation of hydraulic fracture propagation in fractured blocks. Bulletin of Engineering Geology and the Environment 2015;74(3):887–95.

dos Santos JS, Ballestero TP, da Silva Pitombeira E. An analytical model for hydraulic fracturing in shallow bedrock formations. Groundwater 2011;49(3):415–25.

Eriksson KG, Larson SÅ, Haag O. HYDROCK – en ny metod att lagra värme i berg. Technical Report R105:1983. Stockholm, Sweden: Statens råd för byggnadsforskning; 1983. p. 117–23 (in Swedish).

Gu H, Weng X. Criterion for fractures crossing frictional interfaces at non-orthogonal angles. In: 44th U.S. Rock mechanics symposium and 5th U.S.–Canada rock mechanics symposium. American Rock Mechanics Association (ARMA); 2010.

Hart D. A comparison of fracture transmissivities in granite water wells before and after hydrofracturing. Hydrogeology Journal 2016;24(1):21–33.

He Q, Suorineni FT, Oh J. Review of hydraulic fracturing for preconditioning in cave mining. Rock Mechanics and Rock Engineering 2016;49(12):4893–910.

Hellström G, Larson SÅ. Seasonal thermal energy storage – the HYDROCK concept. Bulletin of Engineering Geology and the Environment 2001;60(2):145–56.

Hubbert MK, Willis DG. Mechanics of hydraulic fracturing. Petroleum Transactions AIME 1957;210:153–66.

Ishida T, Chen Q, Mizuta Y, Roegiers J. Influence of fluid viscosity on the hydraulic fracturing mechanism. Journal of Energy Resources Technology 2004;126(3):190–200.

Jaeger J, Cook NG, Zimmerman R. Fundamentals of rock mechanics. 4th ed. Wiley-Blackwell; 2007.

Janiszewski M, Shen B, Rinne M. Hydraulically fractured hard rock aquifer for seasonal storage of solar thermal energy. In: Geomechanics and geodynamics of rock masses: proceedings of the 2018 european rock mechanics symposium. London: CRC Press; 2018.

Jeffrey RG. Asymmetrically propped hydraulic fractures. SPE Production and Facilities 1996;11(4):244–9.

Joshi V. Borewell rejuvenation for sustainability. In: Pickford J, editor. Reaching the unreached – challenges for the 21st century: proceedings of the 22nd WEDC international conference. Loughborough University; 1996. p. 193–4. https://wedc-knowledge.lboro.ac.uk/resources/conference/22/Joshi.pdf.

Kear J, Kasperczyk D, Zhang X, Jeffrey RG, Chuprakov D, Prioul R. 2D experimental and numerical results for hydraulic fractures interacting with orthogonal and inclined discontinuities. In: 51st U.S. Rock mechanics/geomechanics symposium. ARMA; 2017. https://www.onepetro.org/conference-paper/ARMA-2017-0404.

Kresse O, Weng X, Gu H, Wu R. Numerical modeling of hydraulic fractures interaction in complex naturally fractured formations. Rock Mechanics and Rock Engineering 2013;46(3):555–68.

Lamont N, Jessen FW. The effects of existing fractures in rocks on the extension of hydraulic fractures. Journal of Petroleum Technology 1963;15(2):203–9.

Larson SÅ. Hydraulic fracturing in the Bohus granite, SW-Sweden. Test for heat storage and heat extraction. Geothermal Resources Council Transactions 1984;8:447–9. http://pubs.geothermal-library.org/lib/grc/1001215.pdf.

Larson SÅ, Fridh B, Haag Ö. HYDROCK - värmelager i berg. Anläggning av värmeväxlarytor med hjälp av hydraulisk uppspräckning; HYDROCK - metoden. Technical Report Publication B222. Chalmers University of Technology/University of Götenburg; 1983 (in Swedish).

Less C, Andersen N. Hydrofracture: state of the art in South Africa. Applied Hydrogeology 1994;2(2):59–63.

Liebel HT, Huber K, Frengstad BS, Ramstad RK, Brattli B. Thermal response testing of a fractured hard rock aquifer with and without induced groundwater flow. Bulletin of Engineering Geology and the Environment 2012;71(3):435–45.

Lisjak A, Kaifosh P, He L, Tatone BSA, Mahabadi OK, Graselli G. A 2D, fully-coupled, hydro-mechanical, FDEM formulation for modelling fracturing processes in discontinuous, porous rock masses. Computers and Geotechnics 2017;81:1–18.

Liu D, Cui Z, Tian T. The importance of rock fracture mechanics in cap rock stability research for CO_2 storage field. In: 1st workshop under the China-Australia geological storage of CO_2 programme. Canberra, Australia; 2010. http://www.cagsinfo.net/__data/assets/pdf_file/0015/843/session2b-1.pdf.

Liu Z, Chen M, Zhang G. Analysis of the influence of a natural fracture network on hydraulic fracture propagation in carbonate formations. Rock Mechanics and Rock Engineering 2014;47(2):575–87.

McClure MW, Horne RN. An investigation of stimulation mechanisms in enhanced geothermal systems. International Journal of Rock Mechanics and Mining Sciences 2014;72:242–60.

Olasolo P, Juarez MC, Morales MP, D'Amico S, Liarte IA. Enhanced geothermal systems (EGS): a review. Renewable and Sustainable Energy Reviews 2016;56:133–44.

Pine RJ, Batchelor T. Downward migration of shearing in jointed rock during hydraulic injections. International Journal of Rock Mechanics and Mining Sciences and Geomechanics Abstract 1984;21(5):244–63.

Ramstad RK. Ground source energy in crystalline bedrock – increased energy extraction by using hydraulic fracturing in boreholes (PhD Thesis). Norwegian University of Science and Technology; 2004.

Ramstad RK, Hilmo BO, Brattli B, Skarphagen H. Ground source energy in crystalline bedrock-increased energy extraction using hydraulic fracturing in boreholes. Bulletin of Engineering Geology and the Environment 2007;66(4):493–503.

Renshaw CE, Pollard DD. An experimentally verified criterion for propagation across unbonded frictional interfaces in brittle, linear elastic materials. International Journal of Rock Mechanics and Mining Sciences and Geomechanics Abstracts 1995;32(3):237–49.

Rinne M, Shen B, Backers T. Modelling fracture propagation and failure in a rock pillar under mechanical and thermal loadings. Journal of Rock Mechanics and Geotechnical Engineering 2013;5(1):73–83.

Sarmadivaleh M, Rasouli V. Modified Reinshaw and Pollard criteria for a non-orthogonal cohesive natural interface intersected by an induced fracture. Rock Mechanics and Rock Engineering 2014;47(6):2107–15.

Shen B. Development and applications of rock fracture mechanics modelling with FRACOD: a general review. Geosystems Engineering 2014;17(4):235–52.

Shen B, Shi J. Fracturing-hydraulic coupling in transversely isotropic rocks and a case study on CO_2 sequestration. International Journal of Rock Mechanics and Mining Sciences 2016;88:206–20.

Shen B, Stephansson O. Modification of the *G*-criterion for crack propagation subjected to compression. Engineering Fracture Mechanics 1994;47(2):177–89.

Shen B, Stephansson O, Einstein HH, Ghahreman B. Coalescence of fractures under shear stresses in experiments. Journal of Geophysical Research Solid Earth 1995;100(B4):5975–90.

Shen B, Stephansson O, Rinne M, Amemiya K, Yamashi R, Toguri S, Asano H. FRACOD modeling of rock fracturing and permeability change in excavation-damaged zones. International Journal of Geomechanics 2011;11(4):302–13.

Shen B, Stephansson O, Rinne M. Modelling rock fracture processes: a fracture mechanics approach using FRACOD. Dordrecht, the Netherlands: Springer; 2014.

Shen B, Jung Y, Park E, Kim T. Modelling the effect of ice swelling in the rock mass around an LNG underground storage cavern using FRACOD. Geosystem Engineering 2015;18(4):181–98.

Shen B, Shi J, Barton N. An approximate nonlinear modified Mohr-Coulomb shear strength criterion with critical state for intact rocks. Journal of Rock Mechanics and Geotechnical Engineering 2018;10(4):645–52.

Shi F, Wang X, Liu C, Liu H, Wu H. An XFEM-based method with reduction technique for modeling hydraulic fracture propagation in formations containing frictional natural fractures. Engineering Fracture Mechanics 2017;173:64–90.

Starfield AM, Cundall PA. Toward a methodology for rock mechanics modelling. International Journal of Rock Mechanics and Mining Sciences and Geomechanics Abstracts 1988;25(3):99–106.

Sundquist U, Wallroth T. Hydrock - energilager i berg - slutrapport för etapp 1 & 2. Technical Report Publication B349. Chalmers University of Technology/University of Götenburg; 1990 (in Swedish).

Wang Q, Chen X, Jha AN, Rogers H. Natural gas from shale formation – the evolution, evidences and challenges of shale gas revolution in United States. Renewable and Sustainable Energy Reviews 2014;30:1–28.

Warpinski NR, Teufel LW. Influence of geologic discontinuities on hydraulic fracture propagation. Journal of Petroleum Technology 1987;39(2):209–20.

Xie L, Min KB, Shen B. Simulation of hydraulic fracturing and its interactions with a pre-existing fracture using displacement discontinuity method. Journal of Natural Gas Science and Engineering 2016;36:1284–94.

Xu T, Ranjith PG, Au ASK, Wasantha PLP, Yang TH, Tang CA, Liu HL, Chen CF. Numerical and experimental investigation of hydraulic fracturing in Kaolin clay. Journal of Petroleum Science and Engineering 2015;134:223–36.

Xu W, Zhao J, Rahman SS, Li Y, Yuan Y. A comprehensive model of a hydraulic fracture interacting with a natural fracture: analytical and numerical solution. Rock Mechanics and Rock Engineering 2019;52(4):1095–113.

Yoon JS, Zang A, Stephansson O. Numerical investigation on optimized stimulation of intact and naturally fractured deep geothermal reservoirs using hydro-mechanical coupled discrete particles joints model. Geothermics 2014;52:165–84.

Yoon JS, Zimmermann G, Zang A. Numerical investigation on stress shadowing in fluid injection-induced fracture propagation in naturally fractured geothermal reservoirs. Rock Mechanics and Rock Engineering 2015a;48(4):1439–54.

Yoon JS, Zimmermann G, Zang A. Discrete element modeling of cyclic rate fluid injection at multiple locations in naturally fractured reservoirs. International Journal of Rock Mechanics and Mining Sciences 2015b;74:15–23.

Yoon JS, Zang A, Stephansson O, Hofmann H, Zimmermann G. Discrete element modelling of hydraulic fracture propagation and dynamic interaction with natural fractures in hard rock. Procedia Engineering 2017;191:1023–31.

Zangeneh N, Eberhardt E, Bustin RM. Investigation of the influence of natural fractures and in situ stress on hydraulic fracture propagation using a distinct-element approach. Canadian Geotechnical Journal 2015;52(7):926–46.

Zhang X, Jeffrey RG. The role of friction and secondary flaws on deflection and re-initiation of hydraulic fractures at orthogonal pre-existing fractures. Geophysical Journal International 2006;166(3):1454–65.

Zhang X, Jeffrey RG. Reinitiation or termination of fluid-driven fractures at frictional bedding interfaces. Journal of Geophysical Research Solid Earth 2008;113(B08). https://doi.org/10.1029/2007JB005327.

Zhang X, Jeffrey RG, Thiercelin M. Deflection and propagation of fluid-driven fractures at frictional bedding interfaces: a numerical investigation. Journal of Structural Geology 2007;29(3):396–410.

Zhang X, Jeffrey RG, Thiercelin M. Mechanics of fluid-driven fracture growth in naturally fractured reservoirs with simple network geometries. Journal of Geophysical Research Solid Earth 2009;114(B12). https://doi.org/10.1029/2009JB006548.

Zhang L, Zhou J, Braun A, Han Z. Sensitivity analysis on the interaction between hydraulic and natural fractures based on an explicitly coupled hydro-geomechanical model in PFC2D. Journal of Petroleum Science and Engineering 2018;167:638–53.

Zhou J, Chen M, Jin Y, Zhang G. Analysis of fracture propagation behavior and fracture geometry using a tri-axial fracturing system in naturally fractured reservoirs. International Journal of Rock Mechanics and Mining Sciences 2008;45(7):1143–52.

Mateusz Janiszewski is a PhD Candidate in rock mechanics research group at Aalto University in Finland under the supervision of Prof. Mikael Rinne. In his doctoral studies, he focuses on techno-economic aspects of seasonal underground storage of solar thermal energy in hard crystalline rocks and is scheduled to obtain his doctoral degree in 2019. Janiszewski obtained his BSc degree in mining engineering in 2012 at Wroclaw University of Science and Technology in Poland. Then in 2014, he completed the international Master programme called European Mining Course at three universities: Aalto University in Finland, RWTH Aachen in Germany, and TU Delft in the Netherlands. Since then he has been working as a Research Assistant at Aalto University in Finland. His current research interest includes underground thermal energy storage, rock fracture mechanics, geo-risk management, and digital photogrammetry.

Dr. Baotang Shen is a Senior Principal Research Scientist at CSIRO Energy. Dr. Shen obtained his BSc degree in mining engineering in 1985 in China. He obtained his PhD degree in rock mechanics in Sweden in 1993, and then worked with Norwegian Geotechnical Institute (NGI) as a research fellow in 1994–1995. Since 1995, he has been with CSIRO and focused on issues related to highwall mining Geomechanics, mining engineering and mining environment. Dr. Shen is specialised in mining engineering, monitoring instrumentations, numerical modelling, backfill technologies and rock fracture mechanics. Since 2004, he has been leading CSIRO's research team on mine subsidence control and mine remediation, and developed the non-cohesive backfill technology for old mine remediation. The team has completed several major projects funded by Australian Coal Association Research Program (ACARP) and BHP Billiton Illawarra Coal and Queensland State Government on subsidence control and remediation technologies for a number of mines in Australia. Dr. Shen is an influential expert in fracture mechanics modelling. He has initiated and been leading an international collaboration project on coupled fracture mechanics modelling, which is participated by 13 institutes from Germany, Finland, Switzerland, South Korea, China, USA and Australia. He is also the leading author of the recently published book *Modelling rock fracturing processes*.

Mikael Rinne obtained his PhD degree at Helsinki University of Technology in 2008. Since then he has been working as a professor at Aalto University. Before his current position, a number of Finnish and Swedish consulting companies (1988–2008) employed him. His main responsibilities covered research on fracture and rock mechanics related to tunnelling and design of geological disposal of radioactive waste. Since starting as a professor, he has supervised about 100 master theses and four doctoral projects from the start to the end. Rinne's current research interests are in rock engineering, rock fracture mechanics and mining technology. He is the director of the international master programme called European Mining Course at Aalto University.